J Surfact Deterg (2009) 12:73–84
DOI 10.1007/s11743-008-1104-4

ORIGINAL ARTICLE

Partitioning and Localization of Fragrances in Surfactant Mixed Micelles

Elmar Fischer · Wolfgang Fieber · Charles Navarro · Horst Sommer · Daniel Benczédi · Maria Inés Velazco · Monika Schönhoff

Received: 25 March 2008 / Accepted: 15 August 2008 / Published online: 23 December 2008

Abstract The localization and dynamics of fragrance compounds in surfactant micelles are studied systematically in dependence on the hydrophobicity and chemical structure of the molecules. A broad range of fragrance molecules varying in octanol/water partition coefficients P_{ow} is employed as probe molecules in an aqueous micellar solution, containing anionic and nonionic surfactants. Diffusion coefficients of surfactants and fragrances obtained by Pulsed Field Gradient (PFG)-NMR yield the micelle/water distribution equilibrium. Three distinct regions along the $\log(P_{ow})$ axis are identified: hydrophilic fragrances ($\log(P_{ow}) < 2$) distribute almost equally between micellar and aqueous phases whereas hydrophobic fragrances ($\log(P_{ow}) > 3.5$) are fully solubilized in the micelles. A steep increase of the incorporated fraction occurs in the intermediate $\log(P_{ow})$ region. Here, distinct micelle swelling is found, while the incorporation of very hydrophobic fragrances does not lead to swelling. The chemical structure of the probe molecules, in addition to hydrophobicity, influences fragrance partitioning and micelle swelling. Structural criteria causing a decrease of the aggregate curvature (flattening) are identified. ^{2}H-NMR spin relaxation experiments of selectively deuterated fragrances are performed monitoring local mobility of fragrance and leading to conclusions about their incorporation into either micellar interface or micelle core. The tendencies of different fragrance molecules (i) to cause interfacial incorporation, (ii) to lead to a flattening of the micellar curvature and (iii) to incorporate into micelles are shown to be correlated.

Keywords Surfactant · Micelle · Solubilization · Partitioning · Diffusion NMR · Pulsed field gradient NMR · ^{2}H NMR relaxation · Two step model · Fragrance incorporation

Introduction

Surfactant systems build the basic formulation of a variety of water-based consumer products, such as skin care products, cleaners, or liquid washing lotions. In such formulations, surfactant aggregates serve as carrier systems of—predominantly hydrophobic—fragrance molecules. The exact localization of incorporated fragrance molecules in surfactant aggregates is crucial to the understanding of the release dynamics and the interaction with the aggregates, which determines the product properties and quality [1–3]. In addition, incorporated molecules can have a significant influence on the surfactant assembly itself, i.e. by changing the curvature. This was proven for liquid crystalline phases, which can undergo phase transitions upon incorporation of drugs [4] or perfume molecules [5]. On the other hand, the local order and dynamics of the surfactant

Electronic supplementary material The online version of this article (doi:10.1007/s11743-008-1104-4) contains supplementary material, which is available to authorized users.

E. Fischer · M. Schönhoff (✉)
Institute of Physical Chemistry, University of Münster, Corrensstr. 30, 48149 Münster, Germany
e-mail: schoenho@uni-muenster.de

W. Fieber · H. Sommer · D. Benczédi · M. I. Velazco
Corporate R&D Division, Firmenich S.A., P.O. Box 239, 1211 Geneva 8, Switzerland

C. Navarro
Perfumery Division, Firmenich S.A., P.O. Box 239, 1211 Geneva 8, Switzerland

alkyl chains are not necessarily influenced by such additives [6].

In first approximation, the distribution of small organic guest molecules in a micellar surfactant solution is expected to depend mainly on the hydrophobicity or polarity of the guest. Fragrances, for example, are among others characterized by their log(P_{ow}) value, where P_{ow} is the ratio of concentrations of a compound in octanol and water in equilibrium. A number of studies of the micellar solubilization of specific types of guest molecules do exist, while systematic comparisons of a variety of different molecular structures are rare. For example, alcohols have been extensively studied in micellar surfactant solutions [7–12]. For linear or benzyl alcohols, in dependence on alcohol concentration, a maximum in micelle size is found for different types of surfactants. This was interpreted as a transition from a predominant localization in the interface to a localization in the chain region as well [9, 10, 13]. In addition to the guest hydrophobicity, the position of the OH group plays a role [7].

Recent studies of other additives have also shown micellar growth for benzene [14] and for benzyl benzoate [15], respectively, in cationic micelles. Concerning fragrances as guest molecules, their variety of functional groups complicates the finding of general rules governing solubilization and micellar shape changes. A number of authors have studied and compared a set of different fragrances: Tokuoka et al. have determined the distribution coefficients of several fragrances between mixed anionic-nonionic micelles and the aqueous phase [16, 17]. A general trend is that the fraction of fragrance in micelles increases with the hydrophobic character of the fragrance. However, exceptions have been reported for some structures [17].

SAXS has been applied to investigate the influence of probe molecule incorporation into liquid crystalline phases allowing the monitoring of changes of the repeat distances [5, 18–20]. In micellar systems, overall solubility determination or dialysis methods are applied [17, 21]; alternatively NMR spectroscopy yields distinct local information via chemical shifts or spin relaxation rates [6, 22].

In our present approach, we apply Pulsed Field Gradient (PFG) NMR [23–25] to study fragrance incorporation into surfactant micelles. PFG-NMR has already been used as a powerful tool for studies of binding and dynamics in various examples of complex fluids. These include surfactant solutions and microemulsions [26, 27], liquid crystals and membranes [28], associating polymers [29], or colloidal encapsulation systems [30–34]. The approach to employ diffusion studies in solubilization problems was pioneered by Stilbs [35–37]. Measuring fragrance and surfactant diffusion coefficients, the partitioning between micelles and aqueous phase as well as the hydrodynamic radius of the micelles can be determined.

In our present study, we applied this method to a large set of more than twenty different fragrance molecules in order to distinguish overall hydrophobicity and polarity influences from structural ones. Fragrances were chosen such that they cover a very broad range of log(P_{ow}) from about 0.7 to 6, so that the effect of hydrophobicity could be investigated. In addition, the set of fragrances contains compounds with similar log(P_{ow}) values, but rather different chemical structures, such that structure based influences could also be monitored.

The amphiphilic system was a nonionic/anionic surfactant mixture in water, forming a micellar phase at room temperature. The surfactant components were chosen according to their relevance in application, the mixture represented a model system for a basic formulation of an all purpose cleaner (APC) [38, 39]. In this micellar phase, a large variety of fragrances can be dissolved up to concentrations of at least 1 wt.%.

Materials and Methods

Surfactants

The model formulation for an all purpose cleaner consisted of non-ionic and anionic surfactants in water. The non-ionic component is an alkyl ethylene oxide C_nE_m with $n = 12–15$ and $m = 7–8$ (Neodol® 25-7 E, Shell Chemicals, USA) [40, 41].

The anionic component consisted of Na alkylbenzene sulfonate (Na LAS), (MARLON® ARL, Sasol GmbH, Germany). In general, it represented a mixture of regioisomers (main isomer: phenyl ring at 5-position) with different chain lengths ranging from C_{10} to C_{13} and a maximum occurring at C_{11} [42, 43]. In addition, this product contained 14% sodium *p*-toluene sulfonate.

Probe Molecules

In total, 22 fragrances were selected to cover the log(P_{ow}) range from 0.7 to 6 (see table of structures in the Electronic Supplementary Material). They included (in the order of increasing hydrophobicity, with values of log(P_{ow}) given in brackets): vanillin (0.72), 2-phenyl 1-ethanol (1.41), hexanal (2.33), 3-phenyl butanal (2.34), *cis*-6-nonenal (2.88), α-terpineol (2.91), Hedione® (2.92), geraniol (2.97), terpinen-4-ol (3.07), 2,6-dimethyl-2-heptanol (3.24), (E)-4-decanal (3.73), 3-(4-*tert*-butylphenyl)-2-methylpropanal (Lilial®) (3.90), diphenyl ether (3.94), decanal (4.00), (Z)-4-dodecanal (4.52), hexyl (E)-2-methyl-2-butenoate (4.80), *cis*-3-hexenyl salicylate (4.83), dodecanal (4.94),

2-methylundecanal (5.01), hexyl salicylate (5.55), Habanolide® (5.61) and Ambrox® (5.95). The values of $\log(P_{ow})$ of the fragrance molecules were determined by HPLC. The fragrance compounds were obtained from the Firmenich perfumery division. Their purities and identities were controlled by GC, GC/MS and NMR. All fragrance compounds were of high purity (>98%) except Hedione® and Habanolide®. Hedione® is a mixture of *cis* and *trans* isomers (53:47). Habanolide® consists of 4 isomers because of the variation in the position (11 and 12) and configuration (*cis*/*trans*) of the double bond.

Structural Analysis

High resolution liquid state NMR measurements for the characterization of the fragrance compounds were carried out on a Bruker Avance 500 MHz NMR spectrometer, equipped with a 5-mm BBO probe head with gradient coils using standard pulse sequences. GC/MS measurements were done on an Agilent 5973N MSD coupled with an Agilent 6890N GC.

Surfactant Solutions

Non-ionic and anionic surfactant were dissolved in deuterium oxide (99.8 wt.% D_2O, Chemicals&Trading GmbH, Switzerland) and mixed, such that a basic stock solution of 1.74 wt.% anionic and 3 wt.% non-ionic surfactant in D_2O was obtained, i.e., a total surfactant concentration of 4.74%. Samples were prepared by adding 0.5 wt.% of fragrance at $T = 35$ °C under stirring. A vortex was produced in the liquid by slowly increasing the stirring rate, the fragrance was added to the region of highest shear. A homogeneous and stable solution was obtained for all fragrances at a content of 0.5 wt.%. Employing even higher fragrance contents, for some of the probes, a phase separation was observed after a few days. Samples for ^{2}H NMR of selectively deuterated fragrances were prepared in the same way, employing solutions of ultrapure H_2O.

Diffusion Coefficients

NMR experiments were performed at a temperature of $T = 25$ °C using a 400 MHz Avance spectrometer (DMX 400, Bruker). ^{1}H-NMR spectra were recorded employing a liquid state probe head by acquisition of the free induction decay (FID) after a 10° RF pulse. Self-diffusion coefficients were determined by Pulsed Field Gradient (PFG)-NMR employing a probe head with additional gradient coils (Bruker DIFF 30). A stimulated echo sequence with gradient pulses of a duration of $\delta = 2$ ms was employed, and a series of spectra (32) were recorded where the gradient strength g was varied up to a maximum of 1,150 G/cm. The diffusion time was $\Delta = 20$ ms, if not stated otherwise. The procedure for evaluating the self-diffusion coefficient of a species in a PFG NMR data set is to find a peak unambiguously assignable to one molecular component and extract the peak integral or intensity $I(g)$ from each spectrum acquired with a different gradient strength g. The Stejskal–Tanner relation

$$I(g) = I(0)\exp(-kD) = I(0)\exp\left(-(\gamma g\delta)^2(\Delta - \delta/3)D\right) \quad (1)$$

is fitted to the echo decay $I(g)$, where $I(0)$ is the initial amplitude of an echo signal, γ is the gyromagnetic ratio of the protons, and D is the diffusion coefficient.

If peaks contain contributions from more than one component, one must resort to fitting a double exponential to observed echo decays. Thus, mono- or bi-exponential echo decay curves are fitted to the attenuation curves giving one or two diffusion coefficients, respectively. Generally, an accuracy of 5% can be estimated for the measured diffusion coefficients.

Spin Relaxation

^{2}H-NMR spin relaxation experiments were performed using a broad band probe head. The spin–lattice relaxation time (T_1) was measured by inversion recovery experiments [π–τ–π/2-FID]. The spin–spin relaxation time (T_2) was measured by the Carr–Purcell–Meiboom–Gill (CPMG) sequence [π/2–(τ–π–τ)$_n$–*echo*].

Results and Discussion

Nonionic/Anionic Surfactant Solution

^{1}H NMR Spectroscopy

Figure 1 shows the ^{1}H-NMR spectrum of the basic solution of non-ionic and anionic surfactant components in deuterated water. The peak of residual water protons at 4.80 ppm was used for calibration. Numbers displayed in the vicinity of peak maxima indicate chemical shift values of these peaks.

Peaks with different chemical shifts were assigned to the different molecular components present in the solution. The signals between 7 and 8 ppm were attributed to the aromatic protons of the anionic surfactant, while the peak at 3.58 ppm originated from the ethylene oxide protons of the non-ionic surfactant. Well-separated peaks of anionic and non-ionic surfactant components could be distinguished, which is crucial for independent determination of diffusion coefficients of either species. Aliphatic signals

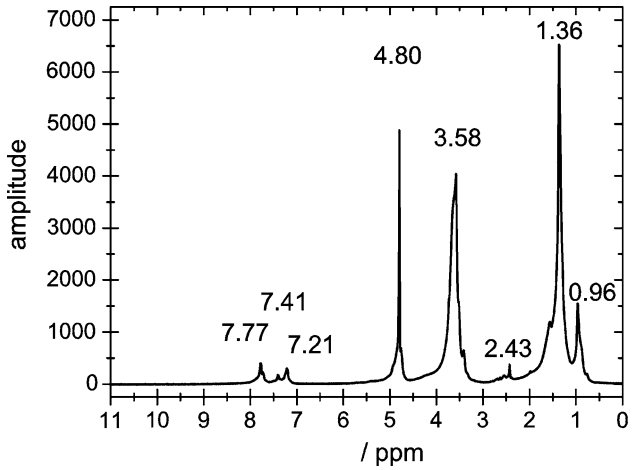

Fig. 1 ^{1}H-NMR spectrum of the basic micellar solution

of surfactants at 1.36 and 0.96 ppm were overlapping signals from both surfactant components.

Self-Diffusion Coefficients

PFG-NMR diffusion experiments were performed on the micellar solution without fragrance. In Fig. 2 echo attenuation curves from diffusion experiments are shown. Echo decays of the peaks of the spectrum in Fig. 1 are displayed using a semi-logarithmic axis versus the generalized diffusion parameter $k = (\gamma G\delta)^2(\Delta - \delta/3)$. Decays of most surfactant resonances were mono-exponential over almost three orders of magnitude. Resonances at 7.41 and 2.43 ppm were overlapped with signals of a small fraction of rapidly diffusing molecules. This was attributed to impurities, which were not incorporated into micelles, and this was accounted for by treating these decay curves by a bi-exponential fit.

The diffusion coefficients of the non-ionic and the anionic surfactant agreed within error. Thus, a common surfactant diffusion coefficient D_s was determined as the average of the diffusion coefficients of the strongest resonances at 7.21, 3.58 and 1.36 and 0.96 ppm of anionic and non-ionic surfactants. The averaged micelle diffusion coefficient was $D_s = (3.2 \pm 0.2) \times 10^{-11}$ m^2/s.

Surfactant diffusion coefficients D_s in micellar solutions are weighted averages of a monomer diffusion coefficient D_1 and the micellar diffusion coefficient D_M according to [35]:

$$D_s = f_M D_M + f_1 D_1, \tag{2}$$

where f_M and f_1 are the fractions of surfactant present in micelles and as monomer in the aqueous phase, respectively. This equation holds for fast exchange between monomeric and micellar surfactant, which is typically the case in micellar solutions [44]. In the present case of a

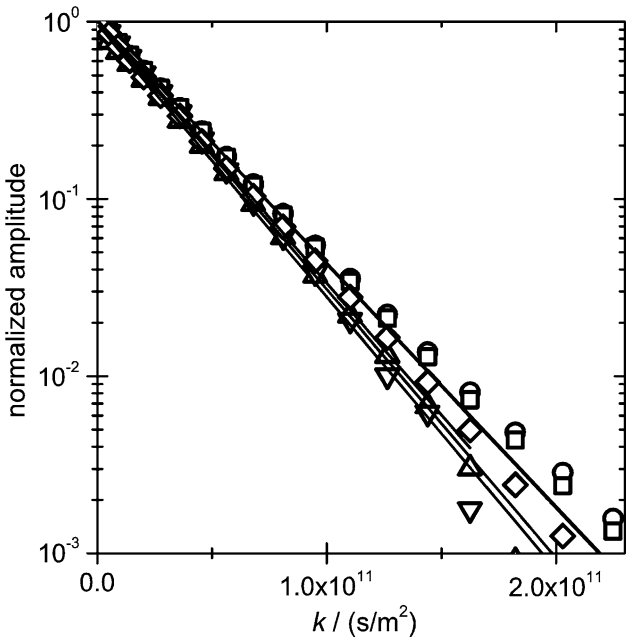

Fig. 2 Self-diffusion echo attenuation curves of micellar solution as a function of the parameter $k = (\gamma G\delta)^2(\Delta - \delta/3)$. *Open triangles* anionic surfactant resonances, *upward triangles* 7.77 ppm, *downward triangles* 7.21 ppm, *circles* non-ionic surfactant resonances, *open circles* 3.58 ppm and *open squares* overlapping non-ionic and anionic surfactant resonances, *open squares* 1.36 ppm, *open diamonds* 0.96 ppm. Fits by mono-exponential decay curves (Eq. 1) are shown as *solid lines*

surfactant solution with a ratio of 1.74 wt.% anionic and 3 wt.% non-ionic surfactant, the concentration of either surfactant was large compared to the critical micelle concentration (CMC). Compared to f_M, the monomer fraction f_1 can be neglected, and it is $D_s = D_M$.

Equivalent Radius

Assuming a spherical shape and employing the Stokes–Einstein equation

$$R_H = \frac{k_B T}{6\pi\eta_0 D_s}, \tag{3}$$

where $k_B = 1.380658 \times 10^{-23}$ J/K, $T = 298.15$ K and $\eta_0 = 1.096 \times 10^{-3}$ Pa s is the viscosity of D_2O at 25 °C, a hydrodynamic R_H of the micelles was extracted. From the diffusion coefficient extracted above, we found $R_H = (6.2 \pm 0.4)$ nm. This radius was larger than that of the maximum size of a spherical micelle, since it exceeded the contour length of the surfactants. Thus, it was concluded that the micelles were non-spherical. Nonionic surfactants of the ethyleneoxide type typically form rod-like micelles [45, 46], thus long rods are the most probable micelle shape also for the present surfactant mixture. For non-spherical aggregates, R_H is an averaged value over all

axes. In the following, we denote the quantity $R_E = R_H$, calculated from the Stokes–Einstein equation, as the 'equivalent radius'. We employed it as a parameter to characterize micelle size, irrespective of the shape.

Fragrance Distribution in Micelle Solution

^{1}H-NMR Spectroscopy

The signals of only 0.5 wt.% of fragrance molecules in micellar solution were clearly visible in the ^{1}H-NMR spectrum. In most cases the fragrances show peaks that are sufficiently separated from those of the surfactant (Fig. 3). A representative ^{1}H NMR spectrum of the surfactant solution with 0.5 wt.% of vanillin is shown as an example in Fig. 3. In comparison to the spectrum of the surfactant mixture (Fig. 1) additional Vanillin signals occur at positions characteristic for the fragrance. Signals at 9.64 and 6.96 ppm do not overlap with surfactant signals, while vanillin signals at 7.39 and 3.86 ppm overlap with surfactant peaks.

Diffusion Measurements

A minimum quantity 0.5 wt.% of fragrance turned out to be sufficient to obtain sufficiently intensive fragrance molecule ^{1}H signals, which were spectrally resolved and well discriminated from surfactant ^{1}H signals, such that diffusion coefficients were obtained with good quality. Echo attenuation curves of surfactant and fragrance spectral lines were mono-exponential. In cases where diffusion coefficients could be obtained from different resonances of the same fragrance, an average value was determined. For surfactants, an average over diffusion coefficients of the strongest resonances of anionic and non-ionic surfactants was taken. Again, as a representative example, the results of self-diffusion echo decays of the micellar solution with 0.5 wt.% of vanillin are displayed in Fig. 4. In addition to echo attenuation curves of surfactant peaks at 7.21, 3.58, 1.36 and 0.96 ppm, decays of vanillin peaks at 9.67 and 6.98 ppm were able to be fitted by mono-exponential decay curves to give an averaged fragrance diffusion coefficient $D_f = (2.6 \pm 0.1) \times 10^{-10}$ m^2/s and an averaged micelle diffusion coefficient of $D_M = (3.1 \pm 0.2) \times 10^{-11}$ m^2/s, respectively.

Surfactant and fragrance diffusion coefficients were determined in a similar manner for in total 22 surfactant solutions containing 0.5 wt.% of a given fragrance from Electronic Supplementary Material, Table 1. A ^{1}H-PFG-NMR experiment was performed for each sample (data not shown). Self-diffusion coefficients are shown in Fig. 5 dependent on log(P_{ow}) of the fragrance molecule present in the solution. As reference values, self-diffusion coefficients of fragrances in water (D_2O) were determined as well.

Diffusion coefficients of fragrances in D_2O (open squares) were on the order of $D = 5 \times 10^{-10}$ m^2/s and correspond to self-diffusion of single fragrance molecules in water. Structural influence and hydrogen bond forming

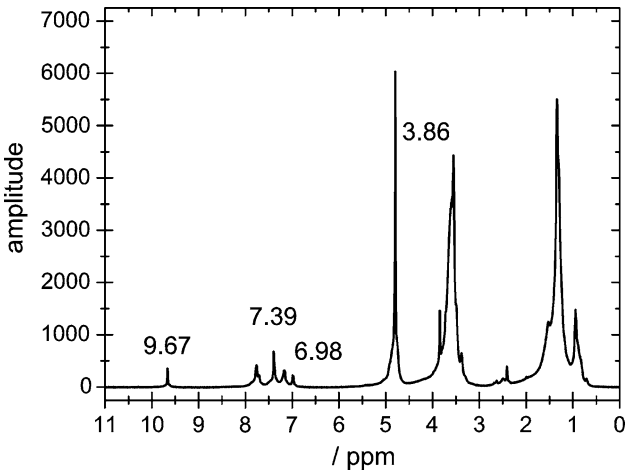

Fig. 3 ^{1}H-NMR spectrum of surfactant solution containing 0.5 wt.% vanillin

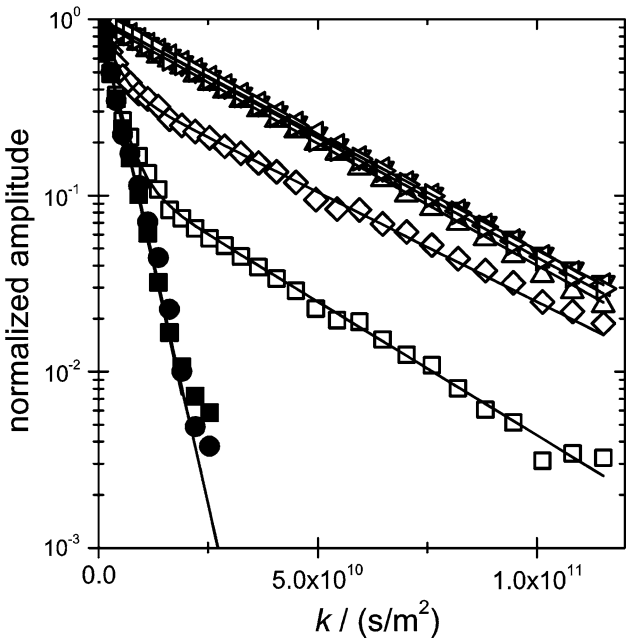

Fig. 4 Self-diffusion echo attenuation curves in surfactant solution containing 0.5 wt.% vanillin as a function of the generalized diffusion parameter $k = (\gamma G\delta)^2(\Delta - \delta/3)$. *Open triangles* surfactant resonances, *upward triangles* 7.19 ppm, *downward triangles* 3.57 ppm, *triangles pointing left side* 1.35 ppm, *triangles pointing right side* 0.96 ppm, *open squares* overlapping surfactant and fragrance resonances, *open squares* 7.41 ppm, *open diamonds* 3.85 ppm, *solid symbols* fragrance resonances, *closed squares* 9.67 ppm, *closed circles* 6.98 ppm. Fits by mono-exponential (Eq. 1) and bi-exponential decay curves are shown as *solid lines*

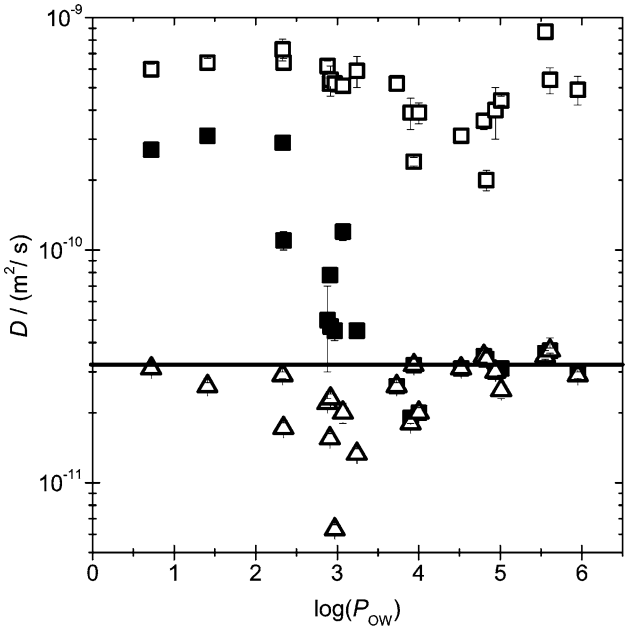

Fig. 5 Self-diffusion coefficients in dependence on log(P_{ow}) of the probe molecule: Fragrance molecule in D_2O (*open squares*); fragrance molecule (*full squares*) and surfactant (*open triangles*) in micelle solution containing 0.5 wt.% of the probe. Fragrance concentration in D_2O is 0.5 wt.% or less, where solubility was limiting. The *solid line* reflects the self-diffusion coefficient of surfactant in the basic surfactant solution

ability might be speculated to be the reason for slightly different diffusion behavior.

Fragrance diffusion coefficients in the micelle solution decreased significantly (see full squares in Fig. 5), which can be attributed to a partial association with micelles: For low log(P_{ow}) molecules, fragrance diffusion coefficients were reduced by a factor of around 2 compared to values for free fragrance in D_2O. In the narrow range from log(P_{ow}) = 2.5 to 3.5, a decrease of diffusion coefficients down to values of the surfactant took place. For even higher log(P_{ow}) values, fragrance and surfactant diffusion coefficients nearly coincide. This proves an incorporation of fragrance molecules into micelles, the degree of incorporation increasing with log(P_{ow}).

The surfactant diffusion coefficient is dependent on the log(P_{ow}) value of the added fragrance: A minimum at intermediate log(P_{ow}) values shows that micelle size was increased in this region due to swelling by fragrance.

Incorporated Fraction

These results can be interpreted by assuming two sites of fragrance molecule localization in the sample: Free molecules diffusing with D_f, the diffusion coefficient of the fragrance molecules in D_2O, and molecules incorporated into the micelle, diffusing with D_M, the diffusion coefficient of the micelle in the mixture. The observed diffusion coefficient D of the fragrance molecule then is a fast exchange average over these two sites, which is weighted by the fraction of molecules in either site. With f_P as the fraction of fragrance molecules incorporated into the micelle, it is:

$$D = f_p D_M + (1 - f_p) D_f = D_f + f_p (D_M - D_f). \quad (4)$$

Thus,

$$f_p = \frac{D_f - D}{D_f - D_M}. \quad (5)$$

Values of f_P, describing the fraction of fragrance incorporated in micelles, were extracted from the respective experimental diffusion coefficients D, D_f and D_M and are given in Fig. 6a. Perfume molecules with log(P_{ow}) below about 2.2 show an incorporation into micelles of about 50–60%, the remaining fragrance molecules diffuse freely in the aqueous phase. Between log(P_{ow}) = 2 and 3.5 a transition region of increasing fragrance content in micelles was reached. Here, the data points scatter significantly, which will be discussed in the next section. Above log(P_{ow}) = 3.5, about all of the fragrance molecules were incorporated in micelles. This result is consistent with the expectation that with increasing hydrophobicity, i.e. increasing log(P_{ow}), the fragrance molecules prefer the hydrophobic environment of the chains and thus the micellar core over the water phase.

Figure 6b gives the micelle-water partition coefficient, which can be defined as the logarithm of the respective fragrance concentrations in micelles (c_{mic}) and in the aqueous phase (c_{wat}), i.e. log(P_{MW}) = log(c_{mic}/c_{wat}). The concentrations are calculated assuming a density of surfactant in micelles that is equal to that of the water. For high log(P_{ow}) values, where f_P is close to one, the errors are too large and data points are not displayed. In the intermediate region of log(P_{ow}) the partitioning into the micelles is reduced as compared to octanol, and the data points scatter significantly.

Swelling of Micelles

The effect of fragrance molecule incorporation on micelle size was evaluated from the diffusion data of surfactant, Fig. 5. Equivalent micelle radii R_E were calculated using Eq. 3 and are displayed in Fig. 7. For small log(P_{ow}) values, equivalent micelle radii increase with increasing log(P_{ow}) and around log(P_{ow}) = 3 a maximum was observed. Here, equivalent radii R_E were up to four times larger than the micelle radius without fragrance. Geraniol with log(P_{ow}) = 2.97 was outstanding, suggesting an equivalent micelle radius R_E of as large as 32 nm. In general, micelle swelling is most pronounced in the

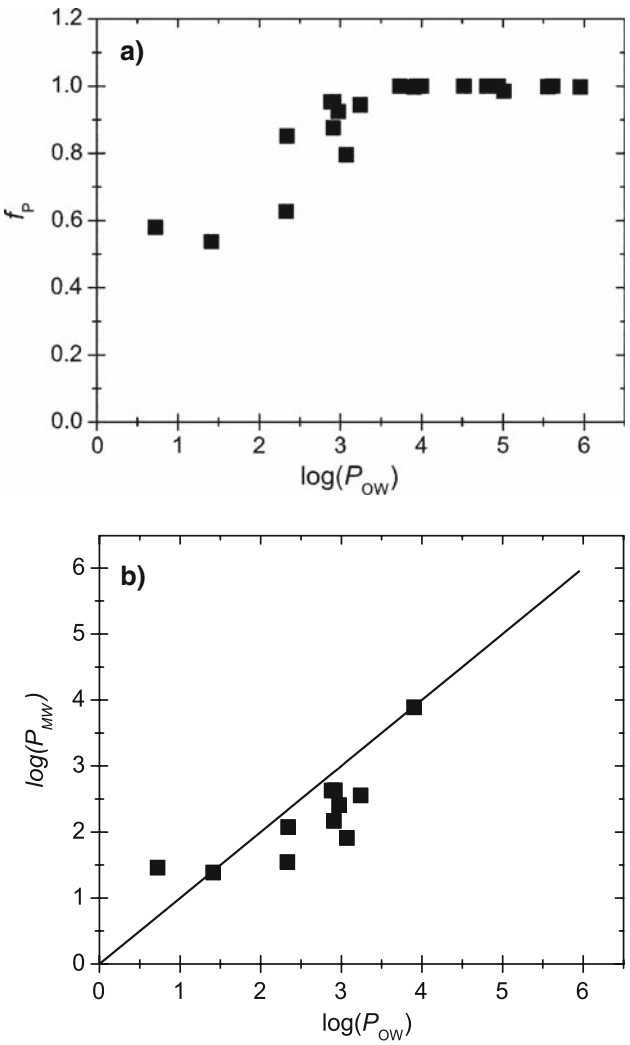

Fig. 6 Fraction of fragrance molecules incorporated in micelles (**a**) and micelle-water partition coefficient (**b**) in dependence on log(P_{ow}). The straight line in (**b**) gives a comparison to log(P_{ow})

medium log(P_{ow}) range. Very hydrophobic fragrances in the high log(P_{ow}) region did not induce swelling of the micelles.

The large scatter of data points in the medium log(P_{ow}) range suggests that log(P_{ow}) is not the only parameter controlling fragrance incorporation and micelle swelling. Relating micelle swelling to the structure of the fragrances, a general trend could be identified, which is illustrated in Fig. 7: Alcohols with a long and partly branched chain (methyl groups or rings) tend, at the same log(P_{ow}), to cause stronger swelling than aldehydes with unbranched alkenyl chains. It is thus concluded that, apart from the log(P_{ow}) value, the exact localization and packing of the molecule in the micelle is relevant.

Generally, a location of a probe molecule associated to a micelle could be (a) in the micelle interior, i.e. the hydrophobic chain region, (b) in the interface or (c) associated to the head groups. Aggregation to the head group from the aqueous phase is not favorable, since it can be expected that this would disturb the hydration shell of the hydrophilic head group. Incorporation into the interface can occur due to the amphiphilic character of most of the fragrances. The fragrance could then act as a co-surfactant. Incorporation into the micellar core is also possible, due to the rather hydrophobic nature of most of the fragrances. This implies that the localization of the fragrance molecules (i.e., in the hydrophobic micelle core or in the interface) is crucial.

^{2}H NMR Spin Relaxation

The question of localization of fragrances in micelles was addressed by determining ^{2}H spin relaxation rates of selectively deuterated molecules, thus monitoring molecular mobility. A sub-set of selectively deuterated fragrances was

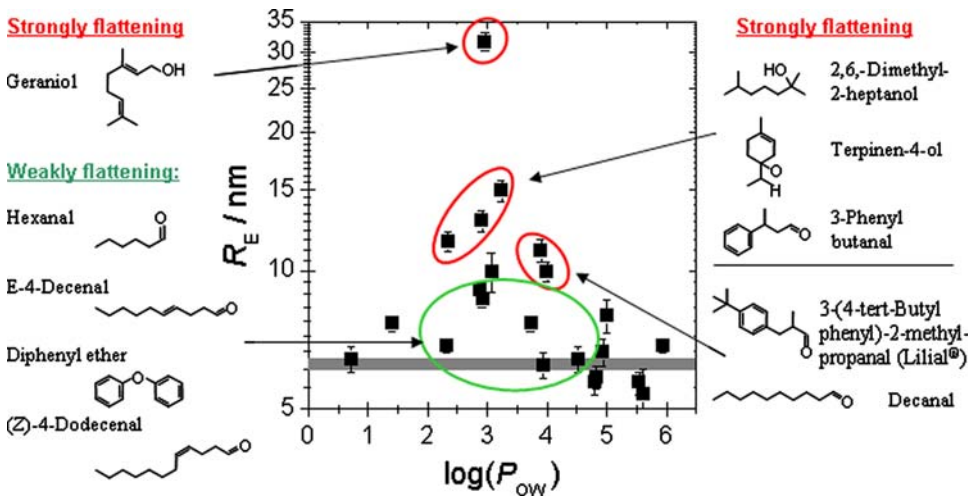

Fig. 7 Equivalent micelle radii of micelles swollen with 0.5 wt.% fragrance as a function of log(P_{ow}). The grey solid line gives the size of micelles without fragrance. Chemical structures of strongly flattening and weakly flattening fragrances in the medium log(P_{ow}) region were given as identified by the equivalent radius R_E of micelles swollen with 0.5 wt.% fragrance

used for this study (respective structures are given in the Electronic Supplementary Material, Table 1, with the position of deuteration indicated). Figure 8 shows ^{2}H spin-lattice and spin-spin relaxation rates R_1 and R_2, respectively, of these fragrances in H_2O. For fragrances with $\log(P_{ow}) > 3.5$ the solubility in water was too low for relaxation measurements.

According to the theory of the two-step model of Wennerström et al. [47], relaxation rates R_1 and R_2 in surfactant systems can be interpreted in terms of molecular motions on two distinctly separated time scales. They introduce a spectral density function

$$J(\omega) = 2\left(1 - S^2\right)\tau_f + 2S^2 \frac{\tau_s}{1 + (\omega\tau_s)^2}, \quad (6)$$

where S is the anisotropy order parameter of the C–D bond relative to the aggregate surface. The fast internal motions such as bond rotations or torsions are characterized by the correlation time τ_f, whereas the slow isotropic reorientations like rotational tumbling and rotational diffusion are described by the correlation time τ_s. Assuming $\omega_0\tau_s \gg 1$, one can show with this spectral density function, that the rate R_1 is dominated by fast segmental motions like bond rotations, occurring with time τ_f. These local motions are usually not much influenced by aggregation. On the other hand, the rate R_2 is strongly influenced by slow isotropic reorientations.

The difference ΔR is then directly proportional to the slow motion correlation time

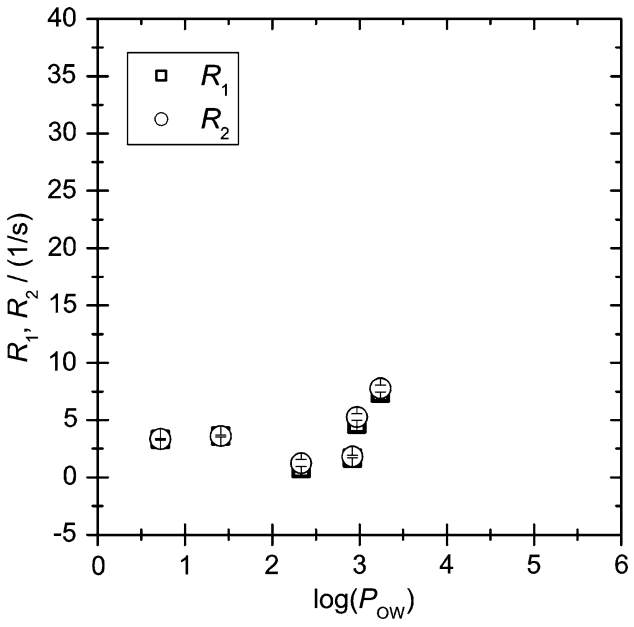

Fig. 8 Spin relaxation rates of fragrances in D_2O. R_1 *open squares*, R_2 *open circles*

$$\Delta R = R_2 - R_1 = \frac{9\pi^2}{20}\chi^2 S^2 \tau_s, \quad (7)$$

where χ is the quadrupolar coupling constant. ΔR can be particularly large if molecules are anisotropically incorporated into amphiphilic aggregates. Then, the order parameter is larger than zero and τ_s describes two superimposed processes, both leading to isotropic averaging: the rotational tumbling of the micelles and the lateral diffusion of the fragrance molecules along the micelle surface.

Relaxation rates of fragrance compounds in water showed the expected behavior of $R_1 = R_2$, see Fig. 8, since isotropic tumbling is fast for non-aggregated molecules. However, the relaxation rates of different fragrances did not coincide. This is probably due to the different structures and positions of deuteration causing a different extent of fast internal motions, and not due to a systematic dependence on $\log(P_{ow})$.

Fast Motions

Figure 9 shows the relaxation rates of deuterated fragrance molecules in micellar solution. Relaxation rates R_1 of fragrance in micelle solution were consistently larger than R_1 of the same fragrance in H_2O. Thus, incorporation of the fragrance molecules into micelles reduces their fast internal motions. If the fragrance is localized in the core region of the alkyl chains, it apparently experiences an enhanced micro-viscosity as compared to aqueous environment. That difference is particularly pronounced with increasing $\log(P_{ow})$ and can be easily explained by the incorporated fraction of fragrance: Due to fast exchange between free and incorporated fragrance, the determined relaxation rates are weighted averages and can be described by an equation analogue to Eq. (4). R_1 for low $\log(P_{ow})$ molecules is then more influenced by the exchange with free fragrances, while R_1 for high $\log(P_{ow})$ is dominated by the viscous micellar core environment of most fragrance molecules.

Slow Motions

With the assumption of similar order parameters, information about the motional correlation time, τ_s, can be obtained from ΔR. It is $\Delta R = 0$ for all fragrances in H_2O, reflecting the regime of extreme narrowing, where isotropic averaging of the molecule is very fast. In micelle solution, for most fragrances, values of ΔR are small, $\Delta R \sim 0$, see Fig. 9. However, largely enhanced values of ΔR were found for geraniol ($\log(P_{ow}) = 2.97$) and for 2,6-dimethyl-2-heptanol ($\log(P_{ow}) = 3.24$). 2-Phenyl-1-ethanol showed a slightly enhanced ΔR, while it was $\Delta R \sim 0$ for the majority of the fragrances.

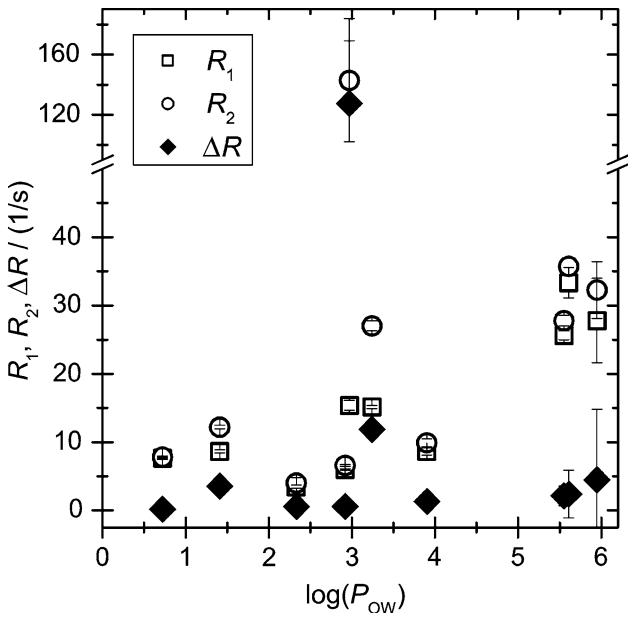

Fig. 9 Spin relaxation rates of fragrances in micellar solution. R_1 *open squares*, R_2 *open circles* and ΔR *closed diamonds*. The values R_1, R_2 and ΔR for geraniol are particularly large, see *broken axis*

According to Eq. 7, ΔR depends on both, the order parameter and the slow motion correlation time, τ_s, which enhances the difference between different localizations. A non-zero ΔR directly implies an anisotropic incorporation of the fragrance with a non-zero order parameter, which means rotational motions are not fast enough to cause isotropic averaging. Thus, the two sets of fragrances with $\Delta R \sim 0$ and $\Delta R > 0$, respectively, can be identified as fragrances incorporated in two different localizations: $\Delta R \sim 0$ with a zero order parameter suggests a localization in an isotropic environment, like the micelle core, or the aqueous solution, which is the case for the majority of fragrances. On the other hand, $\Delta R > 0$ with anisotropic order can only occur with a non-zero order parameter and thus an incorporation of these fragrances into the surfactant layer, i.e. the interfacial region of the micelles. The conclusion is that very hydrophilic or very hydrophobic fragrances incorporate isotropically, while the two fragrances mentioned above (middle log(P_{ow}) region) are localized in an anisotropic environment. This further implies that interfacial incorporation is rather connected to an amphiphilic character of the fragrance molecule, irrespective of its overall hydrophobicity.

Remarkably, fragrances with slow isotropic averaging were only found in the medium log(P_{ow}) region. This implies that the most hydrophobic molecules (log(P_{ow}) > 3.5), which fully partition into the micelles, exhibited fast isotropic averaging, i.e. they are not incorporated into the interface, but rather localized in the micelle core.

Thus, the relaxation data presented here support the varying influences of different fragrances on micelle curvature via a different localization. However, an exact and quantitative analysis of their localizations would require an experimental separation of the parameters τ_s and S by, e.g., field-dependent relaxation experiments.

Generic Structural Rules of Fragrance Incorporation

Comparing results of ^{2}H spin relaxation to those of PFG diffusion, general trends for fragrance localization in micelles on the one hand and fragrance-induced micelle swelling on the other hand were identified.

Low log(P_{ow}) Region

All fragrances from the low log(P_{ow}) region partially incorporated into micelles. Their localization within the micelle was predominantly in the micelle interior, i.e. the alkyl chain region, as concluded from their rotational mobility, see Fig. 10a. However, it has to be noted that due to the large fraction of free fragrance, ΔR is less sensitive to any potential anisotropic localization in the micellar interface for the incorporated fraction. Thus, it might be that the slightly enhanced value of ΔR for phenyl ethanol reflects a partially interfacial incorporation—in contrast to vanillin with a very low ΔR. This could easily be explained by phenylethanol having a slightly more amphiphilic structure than vanillin, such that it can more favorably act as a co-surfactant, while vanillin would incorporate less into a hydrophilic/hydrophobic interface.

High log(P_{ow}) Region

Fragrances from the high log(P_{ow}) region completely incorporated into micelles, as shown in Fig. 10c. In addition, they had a large rotational mobility, as concluded from generally low ΔR values. Both these properties are probably correlated, since a high log(P_{ow}) provides a preferential solubilization in the hydrophobic alkyl chain region. The amphiphilic character of these fragrances was too little pronounced to cause interfacial incorporation. Such hydrophobic probes are incorporated into the core, and do not alter the spontaneous curvature of the surfactant, i.e. they do not show any 'flattening' behavior in spite of the large incorporated fraction, f_p.

Medium log(P_{ow}) Region

The most interesting region certainly was the medium log(P_{ow}) region with a large scatter of data points concerning all properties investigated here: incorporated fraction, swelling of micelles, and finally the rotational

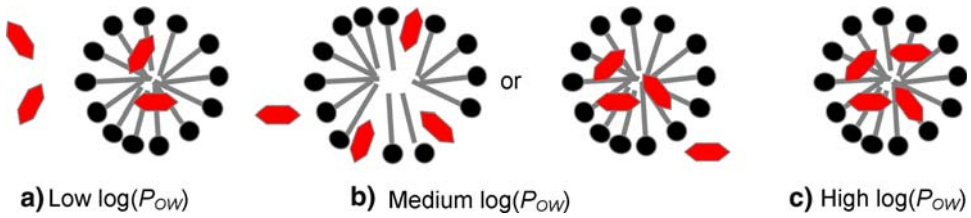

Fig. 10 Model of fragrance incorporation for the low, medium and high log(P_{ow}) region, respectively

mobility of the fragrances. Interesting trends can be identified in this region, which prove the superposition of an influence of the chemical structure with the dependence on log(P_{ow}). Geraniol (log(P_{ow}) = 2.97) and 2,6-dimethyl-2-heptanol (log(P_{ow}) = 3.24) are the compounds which most efficiently caused an increase of micelle size. Since micelle swelling can be attributed to a reduction in spontaneous curvature, these fragrances had a pronounced 'flattening' effect, see Fig. 7. At the same time, these fragrances also showed the largest values of ΔR, i.e. they were most restricted in their rotational tumbling. Both observations can be explained by a preferential incorporation into the interface. These fragrances can be considered as co-surfactant type fragrances and Fig. 7 identifies a larger group of such fragrances. Thus, micellar growth, which was found for simple alcohols [10, 13], is also present for the more complex alcoholic fragrance structures with bulky hydrophobic parts investigated in the present study.

On the other hand, there are those fragrances of the intermediate log(P_{ow}) region which hardly cause any micellar swelling, see the green circle indicating weak flattening in Fig. 7. In this group Hedione (log(P_{ow}) = 2.92) and hexanal (log(P_{ow}) = 2.33) were the two compounds having the lowest values of ΔR. Thus, 'weakly flattening' fragrances can be identified with those that incorporate in the alkyl region and not in the interface. It is mainly aldehydes belonging to this group, while a linear chain aldehyde, decanal, acts more flattening. For decanal, Labows postulated a co-surfactant function [3], which is consistent with our results, too.

There are thus two types of localizations of fragrance molecules of the intermediate log(P_{ow}) region as indicated in Fig. 10b; namely incorporation into the interface or into the core.

There seems to be a correlation with the incorporated fraction in micelles too, which also shows a large scatter of the data points in the intermediate log(P_{ow}) region. Fragrances showing a particularly high incorporated fraction as compared to others of similar log(P_{ow}) are Hedione (log(P_{ow}) = 2.92) and hexanal (log(P_{ow}) = 2.33)—both weakly flattening, i.e. incorporated into the alkyl chain region. On the other hand 3-phenyl-butanal (log(P_{ow}) = 2.34) shows a comparatively low incorporated fraction and is among the strongly flattening fragrances. Thus, interfacial incorporation seemed to be correlated with a slightly reduced partitioning into micelles. However, Geraniol with an extreme flattening effect was an exception to this finding.

In their study of fragrance influence on LC phases of surfactants, Kanei et al. were able to separate their set of fragrances into two groups as well, dependent on their incorporation into the core or the interface of the H_1 phase. Also, their set contained Geraniol, which was identified as incorporating into the interface and decreasing the curvature, consistent with our results [5].

In summary, in this work the incorporation of a large set of different fragrance molecules into surfactant micelles was studied in terms of the fraction of fragrance incorporated into micelles, the size increase of the micelles and the rotational mobility of the fragrance molecules in micelles. Investigated fragrance molecules can be classified by three different regions on the log(P_{ow}) scale. Hydrophilic fragrances with log(P_{ow}) < 2 partially incorporate into micelles, their rotational tumbling is not much hindered, and they can be localized in the micellar core or partially the interface, depending on chemical structure.

Very hydrophobic fragrances with log(P_{ow}) > 4.5 are fully solubilized in micelles, their rotational tumbling is not significantly reduced, and they do not cause micelle swelling. These findings are explained by fragrance localization in the alkyl chain core of the micelles. Irrespective of the chemical structure of the fragrance, in this log(P_{ow}) range, the solubility in the core region is high enough to prevent interfacial incorporation.

In the intermediate log(P_{ow}) range, however, a strong dependence of fragrance partitioning on the chemical structure is superimposing the general dependence on hydrophobicity. Two different sets of fragrances were identified, one of them being bulky structures, predominantly alcohols. Such compounds are extremely hindered in their isotropic motions and lead to micelle swelling. In addition, they tend to show reduced incorporated fractions in micelles which can be attributed to an—at least partial—interfacial incorporation.

Another set of fragrances of intermediate log(P_{ow}) are compounds with long alkenyl chains, several of them being aldehydes. They do not cause micelle swelling, are incorporated to a high degree and do not show significantly reduced rotational dynamics. Accordingly, these compounds are localized in the micelle core.

Thus, employing this large set of different fragrance structures and investigating different aspects of fragrance incorporation into micelles, the influence of structural aspects which superimpose the general dependence on hydrophobicity could be clearly identified.

Acknowledgments The authors would like to thank Christine Vuilleumier for providing the log(P_{ow}) values of the fragrance compounds and Alan Parker as well as Kenneth Wong of Firmenich Corporate Research for helpful discussions.

References

1. Friberg SE (1998) Fragrance compounds and amphiphilic association structures. Adv Colloid Interface Sci 75:181–214
2. Aikens P, Friberg SE (1996) Organized assemblies in cosmetics and transdermal drug delivery. Curr Opin Colloid Interface Sci 1:672–676
3. Labows JN, Brahms JC, Cagan RH (1997) Solubilization of fragrances by surfactants. In: Rieger MM, Rhein LD (eds) Surfactants in cosmetics. Surfactant science series, vol 68. Marcel Dekker, New York, pp 605–619
4. Caboi F, Amico GS, Pitzalis P, Monduzzi M, Nylander T, Larsson K (2001) Addition of hydrophilic and lipophilic compounds of biological relevance to the monoolein/water system. I. Phase behavior. Chem Phys Lipids 109:47–62
5. Kanei N, Tamura Y, Kunieda H (1999) Effect of types of perfume compounds on the hydrophile-lipophile balance temperature. J Colloid Interface Sci 218:13–22
6. Murgia S, Caboi F, Monduzzi M (2001) Addition of hydrophilic and lipophilic compounds of biological relevance to the monoolein/water system II—C-13 NMR relaxation study. Chem Phys Lipids 110:11–17
7. Blokhus AM, Hoiland H, Backlund S (1986) Solubilization of heptanols and α,ω-alkanediols in aqueous-solutions of sodium dodecyl-sulfate. J Colloid Interface Sci 114:9–15
8. Yiv S, Zana R, Ulbricht W, Hoffmann H (1981) Effect of alcohol on the properties of micellar systems. 2. Chemical relaxation studies of the dynamics of mixed alcohol + surfactant micelles. J Colloid Interface Sci 80:224–236
9. Candau S, Zana R (1981) Effect of alcohols on the properties of micellar systems. 3. Elastic and quasi-elastic light-scattering study. J Colloid Interface Sci 84:206–219
10. Zhao GX, Li XG (1991) Solubilization of *n*-octane and *n*-octanol by a mixed aqueous-solution of cationic anionic surfactants. J Colloid Interface Sci 144:185–190
11. Caponetti E, Martino DC, Floriano MA, Triolo R (1996) Application of the small-angle neutron scattering technique to the study of solubilization mechanisms of organic molecules by micellar systems. J Mol Struct 383:133–143
12. Landry JM, Marangoni DG (2008) The effect of added alcohols on the micellization process of sodium 8-phenyloctanoate. Colloid Polym Sci 286:655–662
13. Zhang WC, Li GZ, Shen Q, Mu JH (2000) Effect of benzyl alcohol on the rheological properties of CTAB/KBr micellar systems. Colloids Surf A Physicochem Eng Asp 170:59–64
14. Hedin N, Sitnikov R, Furo I, Henriksson U, Regev O (1999) Shape changes of C(16)TABr micelles on benzene solubilization. J Phys Chem B 103:9631–9639
15. Groth C, Nyden M, Persson KC (2007) Interactions between benzyl benzoate and single- and double-chain quaternary ammonium surfactants. Langmuir 23:3000–3008
16. Tokuoka Y, Uchiyama H, Abe M (1994) Solubilization of some synthetic perfumes by anionic-nonionic mixed surfactant systems. J Phys Chem 98:6167–6171
17. Tokuoka Y, Uchiyama H, Abe M, Christian SD (1995) Solubilization of some synthetic perfumes by anionic-nonionic mixed surfactant systems. Langmuir 11:725–729
18. Vona SA, Friberg SE, Brin AJ (1998) Location of fragrance molecules within lamellar liquid crystals. Colloids Surf A Physicochem Eng Asp 137:79–89
19. Kayali I, Qamhieh K, Lindman B (2006) Effect of type of fragrance compounds on their location in hexagonal liquid crystal. J Dispers Sci Technol 27:1151–1155
20. Uddin MH, Kanei N, Kunieda H (2000) Solubilization and emulsification of perfume in discontinuous cubic phase. Langmuir 16:6891–6897
21. Abe M, Mizuguchi K, Kondo Y, Ogino K, Uchiyama H, Scamehorn JF, Tucker EE, Christian SD (1993) Solubilization of perfume compounds by pure and mixtures of surfactants. J Colloid Interface Sci 160:16–23
22. Suratkar V, Mahapatra S (2000) Solubilization site of organic perfume molecules in sodium dodecyl sulfate micelles: new insights from proton NMR studies. J Colloid Interface Sci 225:32–38
23. Stejskal EO, Tanner JE (1965) Spin diffusion measurements—spin echoes in presence of a time-dependent field gradient. J Chem Phys 42:288–292
24. Stilbs P (1987) Fourier transform pulsed-gradient spin-echo studies of molecular diffusion. Prog Nucl Magn Reson Spectrosc 19:1–45
25. Callaghan PT (1991) Principles of nuclear magnetic resonance microscopy. Clarendon Press, Oxford
26. Söderman O, Stilbs P, Price WS (2004) NMR studies of surfactants. Concepts Magn Reson Part A 23A:121–135
27. Lindman B, Olsson U (1996) Structure of microemulsions studied by NMR. Ber Bunsenges Phys Chem 100:344–363
28. Lindblom G, Orädd G (1994) NMR studies of translational diffusion in lyotropic liquid crystals and lipid membranes. Progr Nucl Magn Reson Spectrosc 26:483–515
29. Thuresson K, Söderman O, Hansson P, Wang G (1996) Binding of SDS to ethyl(hydroxyethyl)cellulose. Effect of hydrophobic modification of the polymer. J Phys Chem 100:4909–4918
30. Adalsteinsson T, Dong WF, Schönhoff M (2004) Diffusion of 77000 g/mol dextran in submicron polyelectrolyte capsule dispersions measured using PFG-NMR. J Phys Chem B 108:20056–20063
31. Rumplecker A, Förster A, Zahres M, Mayer C (2004) Molecular exchange through vesicle membranes: a pulsed field gradient nuclear magnetic resonance study. J Chem Phys 120:8740–8747
32. Bauer A, Hauschild S, Stolzenburg M, Forster S, Mayer C (2006) Molecular exchange through membranes of poly(2-vinylpyridine-block-ethylene oxide) vesicles. Chem Phys Lett 419:430–433
33. Choudhury RP, Schönhoff M (2007) Pulsed-field-gradient NMR study of phenol binding and exchange in dispersions of hollow polyelectrolyte capsules. J Chem Phys 127:234702
34. Fieber W, Herrmann A, Ouali L, Velazco MI, Kreutzer G, Klok H-A, Ternat C, Plummer CJG, Månson J-AE, Sommer H (2007) NMR diffusion and relaxation studies of the encapsulation of fragrances by amphiphilic multiarm star block copolymers. Macromolecules 40:5372–5378
35. Stilbs P (1981) Solubilization equilibria determined through Fourier-transform NMR self-diffusion measurements. J Colloid Interface Sci 80:608–610
36. Stilbs P (1982) Fourier-transform NMR pulsed-gradient spin-echo (FT-PGSE) self-diffusion measurements of solubilization equilibria in SDS solutions. J Colloid Interface Sci 87:385–394

37. Stilbs P (1983) A comparative-study of micellar solubilization for combinations of surfactants and solubilizates using the fourier-transform pulsed-gradient spin-echo NMR multicomponent self-diffusion technique. J Colloid Interface Sci 94:463–469
38. Raney O (1999) Domestic cleaning applications. In: Lange KR (ed) Surfactants. Carl Hanser Verlag, München, pp 171–203
39. Wisniewski K (2006) Speciality liquid household surface cleaners. In: Lai KY (ed) Liquid detergents. Surfactant science series, vol 129. CRC Press, Boca Raton, pp 555–636
40. Murphy RE, Schure MR, Foley JP (1998) Effect of sampling rate on resolution in comprehensive two-dimensional liquid chromatography. Anal Chem 70:1585–1594
41. Swe MM, Yu LYE, Hung KC, Chen BH (2006) Solubilization of selected polycyclic aromatic compounds by nonionic surfactants. J Surfactants Deterg 9:237–244
42. Cavalli L, Landone A, Divo C, Gini G, Galli M, Bareggi E (1976) Identification and structure elucidation of components of commercial linear alkylbenzenes. J Am Oil Chem Soc 53:704–710
43. Das S, Bhirud RG, Nayyar N, Narayan KS, Kumar VV (1992) Chemical-shift changes on micellization of linear alkyl benzenesulfonate and oleate. J Phys Chem 96:7454–7457
44. Evans DF, Wennerström H (1994) The colloidal domain: where physics, chemistry, biology and technology meet. VCH Publishers Inc, New York
45. Nilsson PG, Wennerström H, Lindman B (1983) Structure of micellar solutions of non-ionic surfactants—nuclear magnetic resonance self-diffusion and proton relaxation studies of poly(ethylene oxide) alkyl ethers. J Phys Chem 87:1377–1385
46. Jönströmer M, Jönsson B, Lindman B (1991) Self-diffusion in nonionic surfactant water-systems. J Phys Chem 95:3293–3300
47. Wennerström H, Lindman B, Söderman O, Drakenberg T, Rosenholm JB (1979) C-13 magnetic-relaxation in micellar solutions—influence of aggregate motion on T1. J Am Chem Soc 101:6860–6864

Author Biographies

Elmar Fischer graduated at the University of Ulm, Germany, where he worked on the characterization of high-molecular weight polymer melts with NMR field-gradient diffusometry. He has worked with various NMR diffusion techniques at Massey University, Palmerston North (New Zealand), at the University of Ulm (Germany) and at the University of Münster (Germany), where this work was performed. Currently, he is working on the development of technology for imaging at ultra-high magnetic fields (INUMAC) at the Department of Diagnostic Radiology, University Hospital Freiburg (Germany).

Wolfgang Fieber is working as Scientist in the Corporate R&D Division of Firmenich S.A. in Geneva, Switzerland. He studied chemistry at the University of Innsbruck/Austria and received his Ph.D. in the field of protein folding and NMR spectroscopy. After a postdoctoral stay at the University of Copenhagen (Denmark) he joined Firmenich in 2005, where he works in the NMR analytical service group.

Charles Navarro is Director of Global Technical Development for Surface Care at Firmenich S.A. in Geneva, Switzerland. After his diploma in organic chemistry he graduated in the field of organic radical chemistry at the University of Bordeaux. He joined Akzo Chemicals (later Akzo-Nobel) in the Netherlands where he worked on complexing agents, radical polymer initiators, cross linking agents and chain transfer agents. He started at Firmenich in 2001 where he develops perfume technologies for application in the surface care products.

Horst Sommer obtained his Ph.D. in 1990 from the University of Giessen on optimization, mechanistic and structural aspects of the synthesis of 3-chiral ketones by NMR and X-ray methods. He joined Haarmann & Reimer in 1990 and worked on the structure analysis of flavors and natural products by NMR. In 2003 he started at Firmenich as a Director of the Analytical Service group. His current research interests are in the application of NMR methods to material research topics.

Daniel Benczédi was awarded a Ph.D. in 1995 by the Swiss Federal Institute of Technology ETH in Zurich for a thesis on the thermodynamic properties of starch-water systems. In 1996, he joined Firmenich S.A. in Geneva as a research scientist in charge of the laboratory for encapsulated flavors. In 2003, he was appointed Director of Physical Chemistry and Delivery Technologies in Firmenich Corporate R&D. The field of research of his group covers the physical interactions of flavor and fragrance molecules with polymer- and surfactant-based systems. The resulting know-how is being used to develop novel flavor and fragrance delivery systems answering specific application needs in consumer products of the Food, Bodycare and Household industries.

Maria Inés Velazco is Senior Vice-President of the Corporate R&D Division of Firmenich. She obtained her Ph.D. in Biochemistry at the University of Geneva in 1984 and started working for Firmenich in 1986 after a 2-year postdoctoral position at the Cantonal Hospital of Geneva. She is responsible for scientific research applied to Perfumes and Flavors in the fields of Analytical Chemistry, Materials Science, Sensory Analysis, Psychophysics and Emotion. Her research interests include the domains of physiology, odor and taste perception in humans, discovery and biology of natural chemicals, chemical sensors as well as the brain and emotions.

Monika Schönhoff is professor of Physical Chemistry at the University of Münster (Germany). After her diploma in Physics she graduated in the field of optical spectroscopy of ultrathin organic films at the University of Mainz. Following a postdoctoral stay at University of Lund (Sweden) she started a research group at the Max-Planck-Institute of Colloids and Interfaces in Potsdam-Golm, Germany, working on dynamic NMR studies of organic films. In 2003, she was appointed professor at the University of Münster, where today the expertise of her group is in the studies of the dynamics of encapsulated probe molecules in colloidal carrier systems, as well as ion dynamics and internal properties of polymer electrolytes and polyelectrolyte multilayers, respectively.